Random multiple scattering of ultrasound. II. Is time reversal a self-averaging process?

Arnaud Derode,* Arnaud Tourin, and Mathias Fink
Laboratoire Ondes et Acoustique, Université Denis Diderot-Paris VII, ESPCI-CNRS (UMR 7587), 10 rue Vauquelin, 75005 Paris, France
(Received 14 February 2001; published 28 August 2001)

This is the second article in a series of two dealing with the statistical moments of ultrasonic waves transmitted through a disordered medium with resonant multiple scattering. Second-order moments in time and space are considered here. An ultrasonic pulsed wave is transmitted from a point source to a 128-element receiving array through two-dimensional samples with various thicknesses. The samples consist of random collections of parallel steel rods immersed in water. The scattered waves are recorded, time reversed, and sent back into the medium. The time-reversed waves are converging back to their source and the quality of spatial and temporal focusing on the source is related to the second-order moments of the scattered wave (correlation) in time and in space. Experimental results show that it is possible to obtain a robust estimation on a single realization of disorder, taking advantage of the wide frequency bandwidth. The spatial resolution of the system is only limited by the correlation length of the scattered field, and no longer by the array aperture. As the sample thickness is increased, the quality of focusing saturates, which we believe is linked to the Thouless factor g. In the thickest sample, $g \sim 30$, which is still well above the localization threshold.

DOI: 10.1103/PhysRevE.64.036606 PACS number(s): 43.20.+g, 43.90.+v, 43.35.+d, 73.20.Fz

I. INTRODUCTION

Understanding and modeling wave propagation in a multiple scattering environment has been a subject of interest in a huge variety of domains ranging, e.g., from solid state physics to optics or seismology since multiple scattering can occur with all kinds of waves, whether quantum or classical [1–8]. Studying the statistical moments of the wave amplitude or intensity introduces physical parameters such as the mean free paths, the diffusion constant, or the dimensionless conductance (Thouless factor), which are relevant concepts whatever the type of wave considerered. As to the experimental manifestations of multiple scattering (transition to a diffusive regime, coherent backscattering, long-range correlation, and possibly wave localization), they have also been observed for different kinds of waves [1–17].

In that respect, acoustics brings no new theoretical concept to the study of random multiple scattering, but it does bring original possibilities. Nowadays a typical ultrasonic array consists of 128 programmable wavelength-sized elements that can transmit and receive acoustic waves in a large frequency bandwidth. The wave forms to be transmitted can be easily programmed via a computer interface; as to the received wave forms, the piezoelectric array elements are able to record the field itself, and not only its intensity. Such easiness of use gives way to a number of applications. As an example, it has led to the development of acoustic ''time-reversal mirrors:'' the wave emanating from a source is recorded on a array, time reversed in the computer memory, and sent back in a reverse order by the same array through the same medium [18]. The applications of acoustic time-reversal devices have been widely investigated in the last ten years in the medical field [19], in ocean acoustics [20], in nondestructive testing [21], in chaotic cavities [22,23], and in multiple scattering media [24].

In this paper we will study the transmission and the reversibility of an ultrasonic pulsed wave from a point source to a 128-element array through a multiple scattering slab. This slab is a two-dimensional (2D) sample consisting of a random collection of parallel steel rods immersed in water. Unlike optical wave scattering by suspensions, there is no Brownian motion here: one set of 128 transmitted wave forms corresponds to one realization of disorder, hence there is no ''self-averaging.'' A key question is then to understand what information can be retrieved from the observation of a single realization, and what requires an ensemble average.

The scattered waves are time reversed and sent back through the same slab: the waves tend to focus back to the source. The quality of temporal and spatial focusing is related to the second-order moments of the scattered waves. When the sample thickness becomes larger than the transport mean free path, it will be shown that time reversal gives a robust estimate of the spatial and temporal correlations even on a single realization of disorder, unlike the first-order moment which was studied in the previous article. Moreover the spatial resolution that is achieved by time reversal is only limited by the correlation length of the scattered field, and no longer by the array aperture. For thick samples the quality of focusing saturates as the number of array elements is increased, which we believe is linked to the Thouless factor g. In the thickest sample, $g \sim 30$, which is still well above the localization threshold. Finally, we will emphasize the difference between broadband time reversal and monochromatic phase conjugation, which will be shown to fail in this experiment. This is in agreement with recent work by Blomgren, Papanicolaou, and Zhao [25].

II. SECOND-ORDER MOMENT IN TIME

In this section we study the reversibility of an ultrasonic pulsed wave in a multiple scattering sample. This will lead

*Author to whom correspondence should be addressed. Fax: 33 1 40 79 44 68; Electronic address: arnaud.derode@espci.fr

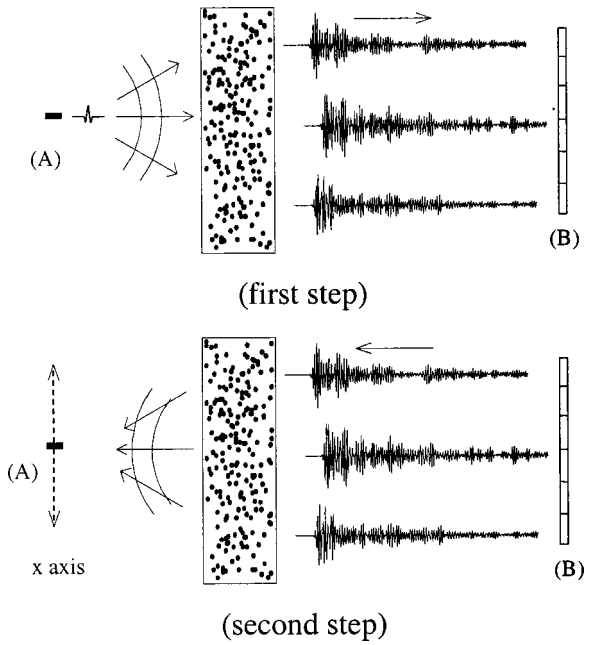

FIG. 1. Time-reversal focusing. In the first step the source (A) transmits a short pulse that propagates through the rods. The scattered waves are recorded on a 128-element array (B). In the second step, N elements of the array ($0<N<128$) retransmit the time-reversed signals through the rods. The piezoelectric element (A) is now used as a detector and measures the signal reconstructed at the source position. It can also be translated along the x axis while the same time-reversed signals are transmitted by B, in order to measure the directivity pattern.

us to investigate the second-order statistics of the scattered field.

A. Experiments

The experimental situation we consider is depicted in Fig. 1. A subwavelength piezoelectric element transmits a short ultrasonic pulse (two cycles of a 3.2 MHz sine wave) that propagates through water and encounters a multiple scattering slab with thickness L. The slab is made of a random collection of parallel steel rods with density 18.75/cm^2 and diameter 0.8 mm (for comparison, the average wavelength in water is 0.47 mm). The receiving array has 128 0.39-mm large elements. The vertical dimensions of the rods and of the array are sufficiently larger than the wavelength to consider the setup as two dimensional. Scattered waves emerge from the sample and the array records 128 time series.

Then the array is used as a ''time-reversal mirror:'' the scattered signals are digitized and recorded into electronic memories, time reversed, and then sent back by the same array through the same scattering medium. One can choose to use the whole array aperture, or any number of elements between 1 and 128. The piezoelectric element that was previously used as a source is now a receiver, and records the wave form generated at the source location after the time-reversal process. It was already shown in earlier studies that the ultrasonic time reversal is a fairly robust operation, unlike one could have expected given the high order of scattering involved and the sensitivity of classical systems to initial conditions, the long-lasting scattered waves ($\sim$200 μs) were found to converge back to the source and recover its original duration (1 μs), with a spatial resolution that was even better than in a homogeneous medium [26].

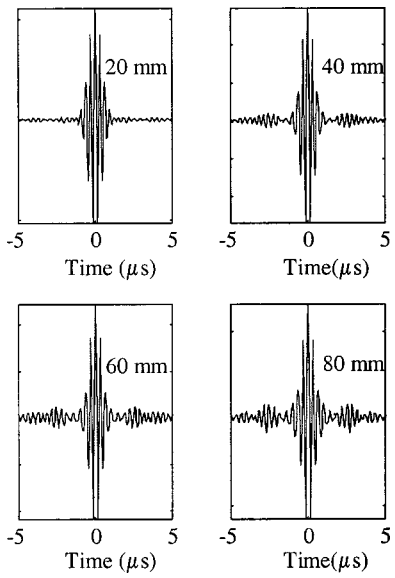

FIG. 2. Signals obtained at the source after time reversing the waves transmitted through thicker and thicker samples.

So it seems that the time-reversal mirror takes advantage of multiple scattering: the energy is spread in time by multiple scattering, but thanks to time-reversal invariance, it can be recompressed to form a short pulse. One could think that the more multiple scattering takes place, the better. We will see that this is not necessarily true.

As an example, the signals that were obtained at the source after time reversal through various scattering samples with the same density are plotted in Fig. 2. Up to a sample thickness $L=20$ mm, the time-reversal process seems to work very well: the scattered wave that spreads over more than 100 μs has traveled back though the sample, undergone multiple scattering in a reverse order, and finally recreated a short peak.

But at $L=40$ mm a sidelobe appears beside the central peak. At $L=60$ and 80 mm this sidelobe is still there, at the same time and with a higher amplitude. It can also be seen in Fig. 3, where the contributions from each array element are represented on a grayscale. For every sample thickness the sidelobe always appears at the same time ($\sim$2.5 μs off the central peak) for all the array elements. This sidelobe is not a mere statistical fluctuation, it is a persistent phenomenon. What is the origin of this sidelobe? Does it have something to do with the resonances in the coherent wave we observed in the previous article?

B. Theoretical analysis and discussion

Let $h(t)$ be the impulse response from the source to one element of the array; by reciprocity $h(t)$ is also the impulse response from this element to the source. Therefore when we transmit a pulse $e(t)$, the signal that is recreated after time

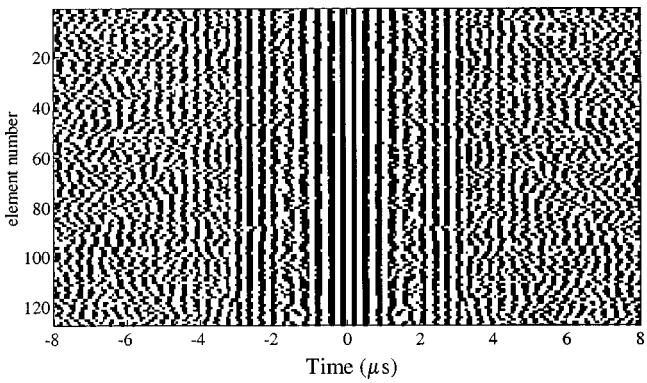

FIG. 3. Time-reversal through $L=80$ mm. Time is in abscissa, and each line on this picture represents the contribution of one array element to the total signal. The grayscale is binary (white=positive, black=negative). The main peak is clearly visible on every contribution at time $t=0$. The sidelobes appear on all elements at the same time, around 2.5 μs off the central peak.

reversal is proportional to $e(t)\otimes h(t)\otimes h(-t)$. For a particular realization of disorder, the impulse response from the source to one array element can be written as

$$h(t)=\langle h(t)\rangle+n(t),$$
$$H(\omega)=\langle H(\omega)\rangle+N(\omega), \tag{1}$$

the brackets denoting an ensemble average, H and N are the Fourier transforms of h and n. In this expression, $\langle h(t)\rangle$ corresponds to the ''coherent'' (ensemble-averaged) impulse response, and $n(t)$ is a zero-mean random contribution which is usually referred to as the ''incoherent'' contribution. In all of the following, a major issue will be the ratio of the coherent to the incoherent part of the scattered waves. For a thin sample, the coherent part is the strongest; but as the sample thickness increases, the incoherent term gains importance. At large L the propagation of the energy tends to be diffusive, as in a random walk, and the incoherent energy can be approximated from diffusion theory.

The signal that is recreated at the source after time reversal is $s(t)=e(t)\otimes h(t)\otimes h(-t)$. $e(t)$ is a deterministic signal, whereas $h(t)$ is random. The statistical average of $s(t)$ is

$$\langle s(t)\rangle=e(t)\otimes\langle h(t)\otimes h(-t)\rangle \tag{2}$$

which can also be expressed in terms of the coherent and incoherent impulse responses:

$$\langle s(t)\rangle=e(t)\otimes\langle h(t)\rangle\otimes\langle h(-t)\rangle+e(t)\otimes\langle n(t)\otimes n(-t)\rangle. \tag{3}$$

Therefore $\langle s(t)\rangle$ will be influenced by $\langle h(t)\rangle$. It was shown in the previous article that the coherent impulse response $\langle h(t)\rangle$ tends to spread in time due to resonant scattering. One could think that the sidelobes in $s(t)$ are due to the same phenomenon. However, the impact of resonance on the signal $s(t)$ is, in our case, negligible.

Indeed, in the Fourier domain, we have

$$\langle S(\omega)\rangle=E(\omega)\langle|H(\omega)|^2\rangle+E(\omega)\langle|N(\omega)|^2\rangle. \tag{4}$$

The first term is the energy conveyed by the ''coherent part'' of the scattered waves, and the second part may be referred to as ''incoherent energy,'' improper as this term may be. For a nonabsorbing slab with thickness L [4], we have

$$|\langle H(\omega)\rangle|^2=e^{-L/l} \text{ and } \langle|N(\omega)|^2\rangle\cong\frac{l^*}{L}, \tag{5}$$

l^* is the transport mean free path, related to the elastic mean free path by

$$l^*=\frac{l}{1-\mu}, \tag{6}$$

with μ the ''average cosine'' of the wave scattered by one rod:

$$\mu=\frac{1}{\sigma}\int\sigma(\varphi)\cos(\varphi)d\varphi. \tag{7}$$

As a physical interpretation, l^* can generally be thought of as a characteristic distance after which the wave has ''lost the memory'' of its initial direction. For isotropic scatterers, $\mu=0$; when forward scattering dominates, $\mu>0$. In the very high frequency regime, $\mu\to1$.

So, the ratio β of the ''coherent'' to the ''incoherent'' energy is

$$\beta=|\langle H\rangle|^2/\langle|N|^2\rangle\approx(1-\mu)\frac{L}{l}e^{-L/l}. \tag{8}$$

This energy ratio can be easily computed as a function of frequency and sample thickness. In the frequency bandwidth 1–5 MHz, its maximum value $\beta_{\max}$ is attained for 2.75 MHz, which was shown to be a resonance frequency. For $L=10$ mm, $\beta_{\max}$ is 0.3, and 0.2 for $L=15$ mm, which is not negligible; yet, as was shown in the previous article, for such thicknesses the coherent wave form does not spread in time. And at larger thickness, $\beta_{\max}$ drops very rapidly (0.13 at $L=20$ mm, 0.01 at $L=40$ mm, and 6×10^{-5} for $L=80$ mm) whereas the sidelobes' amplitude increases with the sample thickness. This shows that when the sample thickness is large enough for the coherent wave form to spread in time, it becomes too weak to contribute significantly to the temporal sidelobes. The physical origin of the sidelobes that appear in the signal obtained by time reversal have to be found somewhere else.

Another possibility that has to be ruled out is that of absorption. The spectrum of the signal obtained at the source after time reversal through $L=80$ mm is plotted in Fig. 4. The temporal sidelobes manifest themselves in the spectrum as quasi-periodic peaks and dips with a frequency interval of $\sim$0.37 MHz. This cannot be explained by attenuation; neither water nor steel present such a frequency dependence in absorption.

Instead, one could think that these sidelobes are a sign of effective irreversibility due to the sensitivity to initial conditions, which becomes more important as the sample thickness (and thereby the order of scattering and the path lengths involved) increases. However, this hypothesis has to be

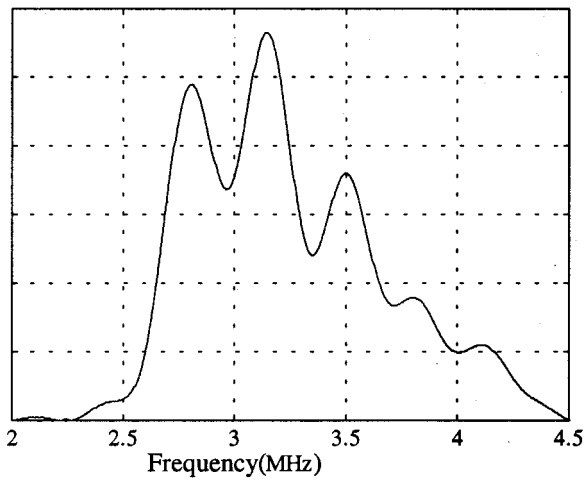

FIG. 4. Spectrum of the signal obtained after time reversal through $L=80$ mm (the signal was windowed between -4 and 4 μs in order to keep only the significant part).

eliminated too. Indeed, the experimental results seem to show no increased sensitivity: two experiments performed in the same conditions within a few minutes yield exactly the same scattered signals, even for the highest orders of scattering, with a correlation coefficient higher than 99.6%.

It would be also tempting to speak of localization: since some frequencies seem to be less and less transmitted through the sample as its thickness is increased, and yet are not absorbed, one could think that they are still trapped within the medium, which would indicate that the diffusion constant is significantly smaller for these frequencies. There is, undoubtedly, what is sometimes referred to as ''weak localization'' in our samples, since the coherent backscattering phenomenon can be observed [27]. However, the elastic mean free path in our frequency bandwidth is of the order of 4 mm, which is ten times as large as the wavelength, so we are still very far from the Ioffe-Regel criterion ($k_0 l \approx 1$) for strong localization.

If the sidelobes in $\langle s(t) \rangle$ are not caused by the spreading of $\langle h(t) \rangle$, then their origin must be a spreading of $\langle n(t) \otimes n(-t) \rangle$. So, in order to explain the growing importance of these temporal sidelobes in the time-reversed signal we propose another hypothesis, based on the existence of correlated scattering paths through the sample. Let us imagine that the signal travels through the sample along a certain number of scattering paths going from one scatterer to the other. Each path has a particular length, which corresponds to a particular arrival time t_i on the receiver. For simplicity, assume that the impulse response from the source to the receiver can be written as a shot noise:

$$h(t)=\sum_i \alpha(t_i)\,\delta(t-t_i). \tag{9}$$

The index i refers to the path number, α is the amplitude associated with a given path (physically speaking, in average, the solution of the diffusion equation gives a ''time of flight'' distribution, and α^2 can be thought of as one realization of the ''time of flight'' distribution).

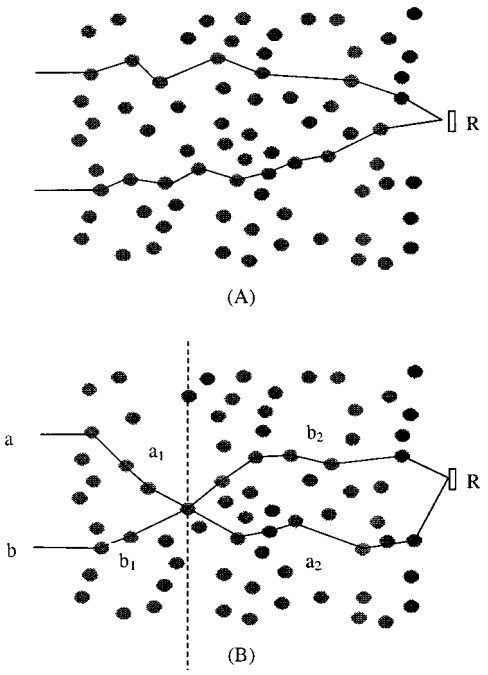

FIG. 5. Sketches of scattering paths arriving on the receiver R. (A): two independent paths. (B): two crossing paths generate four possible arrival times on the receiver. a_1 and a_2 are the travel times corresponding to the first and second part (before and after the crossing) of the path labeled a. The same convention applies to the path labeled b.

Then, after time reversal, the signal recreated will be

$$h(t)\otimes h(-t)=\sum_i \sum_j \alpha(t_i)\alpha(t_j)\,\delta(t-t_i+t_j). \tag{10}$$

This double sum is zero, except at times t such that there exists a pair of scattering paths (i,j) with a time-difference $t_i-t_j=t$. For $t=0$, there is an infinity of such couples: every path, combined with itself, gives rise to a peak with height $\Sigma_i \alpha^2(t_i)$. Roughly speaking, the peak is proportional to the number of significant paths.

Outside the peak, the amplitude of the signal at a time t is linked to the number of path couples (i,j) such that $t=t_i-t_j$. If t_i and t_j can be considered as independent random variables, then there is no correlation between scattering paths, and the difference t_i-t_j has a wide distribution that equals $f(t)\otimes f(-t)$, if $f(t)$ denotes the probability density function for the path length. Then, there is no reason for a particular time t to be more probable than others. But this is no longer the case if the scattering paths are correlated.

A physical reason for the arrival times to be correlated is the growing importance of crossing paths as the sample thickness increases, as well as the ''repulsion'' between scatterers. We give a simple interpretation of the phenomenon in Fig. 5. We keep the idea that the wave is scattered in the sample following every possible path, as a random walker that would bounce from one scatterer to another before getting out of the sample. Each path corresponds to an arrival time t_i in the scattered signal received at some point R. Consider the two paths in Fig. 5(a): they are totally independent

of each other, and since there is no correlation between the scatterers, there is no correlation either between the arrival times t_1 and t_2, as if $n(t)$ was a white "shot noise." But there are also more complicated paths, as the ones drawn in Fig. 5(b). In this example, two paths a and b are crossing in the sample, giving rise to four possible arrival times at point R: t_1, t_2, t_3, and t_4. There are four arrival times, but only two couples of independent paths. Indeed, we have $t_1=a_1+a_2$, $t_2=b_1+b_2$, $t_3=a_1+b_2$, and $t_4=a_2+b_1$: t_1 and t_2 are still independent, as well as t_3 and t_4, but t_1 is correlated with t_3 and t_4, so is t_2.

Now, if every pair (t_i,t_j) forms a couple of independent random variables for $i\neq j$, then the time differences δt will be distributed over a broad interval $[-T,T]$. Whereas if there is a correlation between t_i and t_j $(i\neq j)$, this will not be the case. For instance, if we have $t_1=a_1+a_2$ and $t_3=a_1+b_2$ then $\delta t=b_2-a_2$ will only be distributed over an interval $[-B,B]$, where B is necessarily smaller than T. This implies that the contributions of the crossing paths tend to be gathered around the central peak instead of being spread all over the interval $[-T,T]$.

Naturally this effect becomes more obvious when the number of crossing paths increases. In a random walk, the essential parameter is the transport mean free path l^*. When the sample thickness L is not too large compared to l^*, most paths going to the receiver do not cross one another. But as the sample thickness increases, the paths traversing the slab get more and more intricate and the probability of crossing increases, inducing a correlation in the arrival times.

When we use a 128-element array, the total signal recreated at the source writes

$$r(t)=\sum_{k=1}^{128} h_k(t)\otimes h_k(-t)=\sum_{k=1}^{128}\int h_k(\theta)h_k(t+\theta)d\theta, \tag{11}$$

hence $r(t)$ can be viewed as a statistical estimate of the time-autocorrelation function of the scattered waves $\langle h(\theta)h(t+\theta)\rangle$. If $h(t)$ was actually a decorrelated series of impulses, then $\langle h(\theta)h(t+\theta)\rangle$ should fall to zero. The existence of persisting temporal sidelobes in the time-reversal experiment at large thickness is an indication of a correlation in the arrival times, and we interpret this correlation as a consequence of the growing number of crossing paths. As a result, the coherence time of $e(t)\otimes h(t)$ is larger than the duration of the initial pulse $e(t)$.

In three samples with the same scatterers' density and different thicknesses (40, 60, and 80 mm), the sidelobe appears exactly at the same time: $\sim$2.5 μs from the main peak, which corresponds to a path length difference of 3.8 mm in water. We think this value is probably related to the average distance between a scatterer and its closest neighbor. Indeed, among all possible correlated paths, the simplest case is "recurrent scattering:" the wave simply bounces between two scatterers. Recurrent scattering is most likely to occur between close scatterers. In a two-dimensional set of independent points picked at random uniformly with an average density per unit surface n, the probability density function for the distance z between closest neighbors is given by

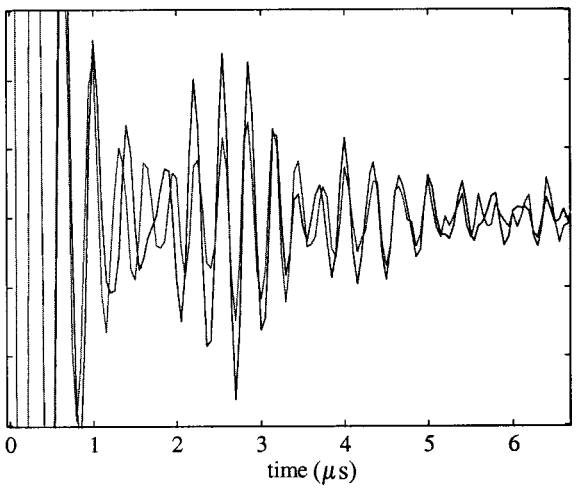

FIG. 6. signals obtained after time reversal in transmission (thin line) and in backscattering (thick line). The time origin is at the central peak, whose amplitude has been saturated to enhance the secondary sidelobe.

$2n\pi z\exp(-n\pi z^2)$, and its mean value is 1.15 mm for $n=0.1875\,\mathrm{mm}^{-2}$. But in the media we studied, as in a real gas, the scatterers' positions are not independent: since they have a radius of 0.4 mm, the scattering centers cannot be closer than 0.8 mm. Moreover, when the samples were fabricated, holes were drilled into two parallel plates to maintain the rods. In order to be sure that the close holes would not accidently overlap, an exclusion distance was added: the holes' positions were picked at random and uniformly, but could not be closer than 1.5 mm. This "repulsion" induces a correlation between the position of the scattering centers. Taking this into account, the mean value for the distance z between closest neighbors is 1.79 mm, which yields a typical time of 2.4 μs for the wave to bounce between two close scatterers.

We believe that recurrent scattering is the physical origin of the secondary sidelobes, and that the position of the main sidelobe (2.5 μs off the central peak) is related to the mean distance between close scatterers.

For a small sample thickness, most scattering paths do not cross each other. On the contrary, as the sample thickness increases, the probability of crossing and of recurrent scattering grows, and so does the amplitude of the temporal sidelobe.

Interestingly, this phenomenon can also be shown in a backscattering configuration, for $L=80$ mm. The setup is almost the same as in Fig. 1, except that the source is on the same side as the array (in fact, one element of the array is used as a source). If we time reverse the first 200 μs of backscattered signals, there are no persistent sidelobes. But if we time reverse the next 200 μs, corresponding to longer and more intricate scattering paths, the same sidelobe appears exactly at the same time as in the transmission configuration (Fig. 6).

The backscattered waves that arrive between 200 and 400 μs after the first reflection have traveled between 300 and 600 mm through the sample, i.e., between 60 and 120 times the transport mean free path. For such long scattering paths,

the wave has lost the memory of its initial direction and it is therefore logical that there is no difference in the statistics of the arrival times in the backward and in the forward direction. Once again, the path lengths involved ($60-120l^*$) are very large compared to the sample thickness ($L\sim 16l^*$); hence they are likely to be tortuous, to cross one another, to include loops and recurrent scattering, all kinds of phenomena that induce correlation in the arrival times.

Yet this raises an apparently troublesome question. Even if the scatterers are correlated and recurrent scattering occurs, energy conservation and time-reversal invariance should still hold. Yet the experimental results show that the secondary sidelobes are the same in the forward and in the backward direction, which seems to indicate that even if we had a perfect time-reversal device that would surround the scattering medium completely, the signal obtained after time reversal would still have a sidelobe, and thus time-reversal invariance would be broken. If, as we said before, we rule out absorption and sensitivity to initial conditions, we have to look for another explanation.

The temporal sidelobes appear as ''missing frequencies'' in the spectrum (Fig. 4). Such dips are visible in the transmitted wave and in the last part (longest and least energetic paths) of the reflected wave. If we could have a perfect time-reversal device and time-reverse the transmitted as well as the reflected waves, there would be two possible results. Either time-reversal works and recreates the original pulse (without the sidelobes) and that would mean that the ''missing frequencies'' are in the early part of the reflected waves, only they are hidden by statistical fluctuations; or it does not work, and that would mean that the ''missing frequencies'' are still trapped somewhere within the sample. For the time being, we cannot bring an experimental answer to this question.

III. SECOND-ORDER MOMENT IN SPACE

In the previous section we were interested in the signal that was recreated at the source after time reversal. We are now going to study the field outside the source position, in order to investigate how well the beam is focused, and what are the parameters that influence the quality of spatial focusing.

A. Experiments

To that end, the same time-reversed signals are continuously retransmitted by N elements of the array ($0<N<128$), while the detector is translated parallel to the array (Fig. 1). Thus a two-dimensional set of signals $s(x,t)$ is measured, where t denotes time and x the distance from the source. The array aperture (i.e., the number N of active elements) can be easily varied from 1 to 128.

From this set of signals there are several ways to form a beam pattern. Commonly in ultrasound physics, drawing the directivity pattern $d(x)$ consists in keeping the maximum value for each position:

$$d(x)=\max\{|s(x,t)|\}. \tag{12}$$

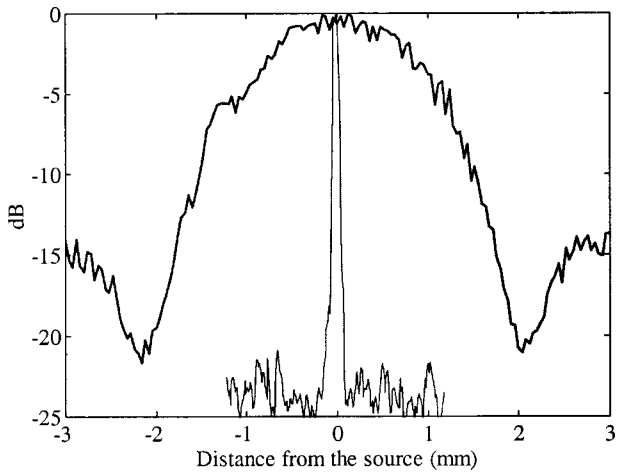

FIG. 7. Directivity pattern of the time-reversed waves around the source position, in water (thick line) and through the rods (thin line), with a 16-element aperture. The sample thickness is $L=40$ mm. The -6 dB widths are 0.8 and 22 mm, respectively.

It is also possible (and easier to handle in the theory) to retain the value at time $t=0$ (i.e., the arrival time of the peak)

$$d(x)=s(x,0). \tag{13}$$

Alternatively, a frequency analysis via a Fourier transform gives the beam pattern for each frequency:

$$d(x,\omega)=\int s(x,t)e^{-j\omega t}dt. \tag{14}$$

As a typical result, Figs. 7 and 8 present experimental directivity patterns [as defined in Eq. (12)] that were obtained through a 40-mm-thick sample. Two points are clearly demonstrated by these results.

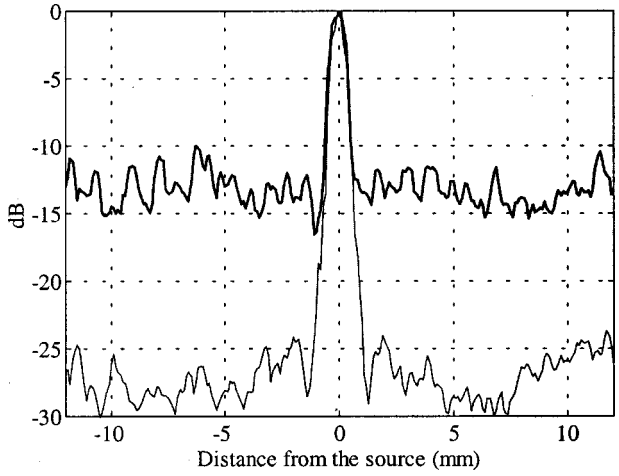

FIG. 8. Directivity pattern of the time-reversed waves around the source position through $L=40$ mm, with 128 transducers (thin line) and 1 transducer (thick line). The -6 dB resolutions are 0.84 and 0.9 mm, respectively.

(1) Figure 7 shows that the resolution (i.e., the beam width around the source) is significantly finer than in the absence of any scattering medium. In Fig. 7 the resolution is 30 times finer and the background level is always below -20 dB.
(2) Figure 8 shows that the resolution seems to be independent of the array aperture: even with only one transducer doing the time-reversal operation the quality of focusing is quite good and the resolution remains approximately the same with an aperture 128 times larger. However, the background level strongly depends on the number of elements.

We will try to understand and interpret these results.

B. Interpretation

A short explanation for this surprising effect is that, due to the presence of the scatterers, high spatial frequencies that would have been lost otherwise are redirected towards the array. In other words, when the time-reversed waves propagate back, the medium acts as a lens that focuses the signal on the source; the angular aperture of that pseudo-lens is larger than that of the array alone, hence the improvement in resolution.

Another argument, based on reciprocity, can be developed to account for this result. Imagine that the time-reversal operation is performed on one array element R. As usual, when a point source P_1 sends a pulse, the detector R records the scattered signal $h_1(t)$. The time-reversed signal is sent back by R and propagates through the same medium. At the source position, as usual, the recreated signal is

$$h_1(-t)\otimes h_1(t). \tag{15}$$

If we consider another observing point P_2, somewhere around the source, and denote by $h_2(t)$ the propagation impulse response from R to P_2, the signal recreated in P_2 is

$$h_1(-t)\otimes h_2(t). \tag{16}$$

Now, due to reciprocity, the source P_1 and the receiver R can be exchanged: in other words, $h_1(t)$ is also the signal that would be received in P_1 if the source was in R. Therefore we can imagine a situation in which R is a source, and the transmitted wave field is observed at two points P_1 and P_2 on the other side of the sample, separated by a distance $x_{12}=P_1P_2$.

Using Eq. (13) to define the directivity pattern, we have

$$d(x_{12})=\int h_1(t)h_2(t)dt. \tag{17}$$

Alternatively, the frequency definition of the directivity pattern [Eq. (14)] would give

$$d(x_{12},\omega)=H_1^*(\omega)H_2(\omega). \tag{18}$$

Both definitions are related since we have

$$d(x_{12})=\int d(x_{12},\omega)d\omega. \tag{19}$$

Whatever the definition of the directivity pattern, what matters is that, in average, both $d(x_{12})$ and $d(x_{12},\omega)$ are related to the spatial correlation function of the wave field transmitted through the slab, i.e., $\langle H_1(\omega)H_2^*(\omega)\rangle$.

So, interestingly, the directivity pattern can be viewed as a statistical estimator of the spatial correlation function. In that sense, the spatial resolution of the system (i.e., the -6 dB width of the directivity pattern) is simply an estimate of the coherence length of the wave field transmitted through the scattering sample. Considering the spatial resolution as a measure of the coherence length of the field transmitted through the random sample permits us to interpret a number of results, as we will see in the next paragraphs. To begin with, we will only consider the case when the time-reversal operation is performed on a single element.

C. Increasing the sample size

The key to the directivity pattern of the time-reversed beam is the spatial correlation function of the wave field $\langle H_1(\omega)H_2^*(\omega)\rangle$, which will strongly depend on the ratio of the coherent to the incoherent part of the scattered waves.

For relatively thin samples (L comparable to the transport mean free path l^*), the coherent wave front dominates, therefore the correlation length of the transmitted field will be large, and no focusing is possible when using a single element on the array. On the contrary, as the sample thickness increases, the coherent wave front vanishes and the ''incoherent'' term dominates: the correlation length of the transmitted field diminishes and the resolution is finer. The problem is to evaluate $\langle H_1(\omega)H_2^*(\omega)\rangle$ more precisely as a function of the sample thickness.

In 1986, Shapiro [28] studied the correlation of the intensities $I_1=|H_1|^2$ and $I_2=|H_2|^2$ transmitted in two points:

$$C_{12}=\frac{\langle I_1I_2\rangle-\langle I_1\rangle\langle I_2\rangle}{\langle I_1\rangle\langle I_2\rangle}. \tag{20}$$

He gave a theoretical prediction in the case of a point source in an infinite medium:

$$C_{12}=\mathrm{sinc}^2(k_0x_{12})e^{-x_{12}/\ell^*}, \tag{21}$$

x_{12} is the distance between the observing points and k_0 the wave number. Now, to evaluate $\langle H_1H_2^*\rangle$, we begin by separating the coherent field from the zero-mean incoherent contributions, as we did in Eq. (1):

$$H_1=\langle H_1\rangle+N_1, \tag{22}$$

$$H_2=\langle H_2\rangle+N_2.$$

The ω dependence has been omitted. This yields

$$\langle H_1H_2^*\rangle=\langle H_1\rangle\langle H_2^*\rangle+\langle N_1N_2^*\rangle. \tag{23}$$

In the weak scattering limit we have

$$|\langle N_1 N_2^* \rangle|^2 \approx C_{12} \langle |N_1|^2 \rangle \langle |N_2|^2 \rangle. \quad (24)$$

Moreover, if the ''incoherent'' energy is well described by the diffusion equation, we have

$$\langle |N_1|^2 \rangle = \langle |N_2|^2 \rangle \approx \frac{l^*}{L}. \quad (25)$$

Besides, the ''coherent'' part of Eq. (23) is simply the energy of the coherent wave field, $|\langle H \rangle^2| = \exp(-L/l)$. Finally, we have

$$\langle H_1 H_2^* \rangle \approx e^{-L/l} + \frac{l^*}{L} \sqrt{C_{12}}. \quad (26)$$

The first term on the right-hand side does not depend on the distance x_{12} between the observing points: it corresponds to the coherent wave-front contribution that is present on every receiving point, with an infinite coherence length. But its energy decreases exponentially with the sample thickness. On the contrary, the second term depends on x_{12}: it vanishes as soon as x_{12} is greater than the wavelength. Since this term varies in $1/L$, it gets larger than the coherent term as L increases.

We have argued earlier that the spatial resolution of a time-reversal device essentially depends on the correlation length of the scattered wave field: the shorter the coherence length, the finer the resolution. If the sample thickness and the mean free path are such that $\langle H_1 H_2^* \rangle$ is dominated by the coherent term, the resolution will be poor. Whereas the finest resolutions should be attained when the incoherent term dominates.

Physically, in the time domain, this means that for small thickness the transmitted wave is an almost perfectly coherent wave front that does not last a very long time. When doing the time-reversal operation with a single element R, there will be no focusing.

But at large thickness, the transmitted wave forms have a very small correlation length and a very long duration. When doing the time-reversal operation, even with a single element R, we obtain a very fine focusing because the impulse responses h_1 (from R to the source P_1) and h_2 (from R to a point P_2 near the source) are rapidly decorrelated, even if P_1 and P_2 are close. Shapiro's result sets a limit: the minimum coherence length for the ''incoherent'' contribution is the wavelength. It is therefore, as we saw experimentally, possible to focus a pulsed wave through a strongly scattering medium even with only one element, with a resolution of the order of the wavelength.

For intermediate situations ($5l^* > L > l^*$), the directivity pattern will be a combination of coherent and ''incoherent'' terms, thus giving an intermediate resolution. Equation (26) could be integrated over the frequency spectrum to yield a theoretical prediction that can be compared to the experimental results obtained in the time domain. However, it should be noted that the validity of Eq. (26) is highly questionable for such values of L, for which the coherent part is of the same order than the incoherent part: the basic arguments are still valid (the field can always be split into a coherent and an incoherent contribution), but the incoherent intensity can no longer be evaluated by l^*/L since the diffusion approximation does not hold. A more complicated expression derived from radiative transfer theory could be introduced instead of the diffusion approximation. Anyway, to our knowledge, there is no simple theoretical prediction of the ''incoherent energy'' $\langle |N|^2 \rangle$ that would be valid from $L = 0$ to $L \to \infty$.

When L is large enough compared to l^* to use the diffusion approximation, Eq. (26) gives a more reliable prediction of the -6 dB resolution. Since the average wavelength λ is significantly smaller than the transport mean free path l^*, the resolution essentially depends on the sinc term. Its -6 dB width is 0.29 mm for a central frequency 3.2 MHz. Experimentally, the best resolution we could achieve through $L = 40$ mm was 0.45 mm, but it was measured with a 0.39 mm transducer, which tends to overestimate the size of the focal spot.

D. Time reversal versus phase conjugation

Phase conjugation is a monochromatic version of time reversal. An important point must be emphasized: Eq. (26) gives only an *average* result of the directivity achievable by time reversing the scattered wave on a single element at a single frequency. In order to have a sensible prediction of what can be expected in an experiment, i.e., on a single realization of disorder, one has to evaluate the statistical fluctuations of the directivity pattern $d(x_{12}, \omega) = H_1 H_2^*$.

Precisely, in order to evaluate the background level of the directivity pattern, the mean value of $d(0, \omega)$ has to be compared to the standard deviation of $d(x_{12}, \omega)$ for a distance x_{12} larger than a few wavelengths, i.e., we compute the ratio of the fluctuation of the directivity pattern (outside the source) to the amplitude at the source. Separating H_1 and H_2^* into a coherent and an incoherent term, we obtain after a few lines:

$$\frac{(\text{fluctuation})}{(\text{amplitude at the source})} = \frac{\sqrt{1+2\beta}}{1+\beta}, \quad (27)$$

β denotes the ratio of the coherent to the incoherent energies:

$$\beta = |\langle H \rangle|^2 / \langle |N|^2 \rangle. \quad (28)$$

When the sample thickness is small, or of the order of the mean free path, the coherent energy dominates, i.e., $\beta \gg 1$: then the fluctuation is negligible. But in that case, as we have seen, there is no focusing. The element that performs the phase conjugation will generate a field that does not vary from one realization to the other (so it can be predicted with a good accuracy) but that field is not focused on the source.

On the contrary, when the sample thickness is larger than the transport mean free path, the incoherent term dominates, $\beta \to 0$, and the result is that the fluctuation of the field around the source is of the same order than the amplitude refocused at the source. So there is, on average, a focusing on the source; but on a given realization of disorder, the fluctuation is so large that the focusing is not visible. This has an important consequence: a phase conjugation experiment per-

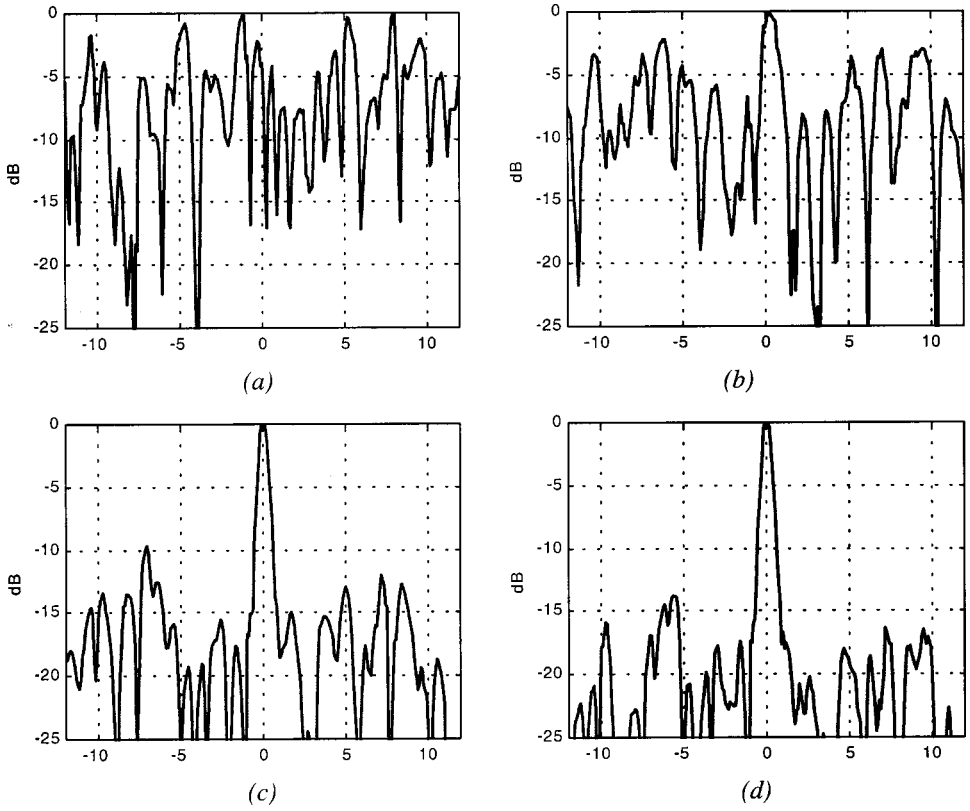

FIG. 9. Directivity patterns obtained with a single element through $L=40$ mm (abscissa: distance from the source in mm). (a) phase conjugation at the center frequency, (b) time reversal using 10% of the transducer bandwidth, (c) time reversal using 40% of the bandwidth, and (d) time reversal using the full bandwidth.

formed on a single element in a multiple scattering sample cannot work. This is illustrated in Fig. 9, which displays the directivity pattern obtained by phase conjugating the central frequency (3.2 MHz) component of the scattered wave through $L=40$ mm. There is no focusing on the source: phase conjugation does not work in such a situation.

However, when we do a real time-reversal experiment, we make use of all the frequency components of the incoming pulse, as if we were doing a phase conjugation operation over a large spectral bandwidth. This is the reason why it is possible, as we have seen, to refocus a wave even with a single element performing the time reversal.

Indeed, in order to achieve a good focusing on one realization of disorder (i.e., on a given and fixed scattering medium), we have to reduce the statistical fluctuation of the directivity pattern. By doing wideband time reversal instead of monochromatic phase conjugation, the final directivity pattern is an average of the directivity patterns at each frequency.

The key issue is to know whether the data that are being averaged are correlated or not. Let $\delta\omega$ be the spectral correlation length of the scattered waves and $\Delta\omega$ the total bandwidth. Then there is $\Delta\omega/\delta\omega$ uncorrelated information (or spectral ''information grains'') in the frequency bandwidth, and the fluctuation is expected to be reduced by a factor of $\sqrt{\Delta\omega/\delta\omega}$.

The same analysis can also be made in the time domain. Indeed, second-order moments in time and frequency are related by the Wiener-Kinchin theorem:

$$\int \langle H(\omega)H^*(\omega+\delta\omega)\rangle d\omega = \int \langle |h(t)|^2\rangle e^{j\delta\omega t} dt. \quad (29)$$

In other words, the spectral correlation function (averaged over the frequency bandwidth) is the Fourier transform of the ''time of flight'' distribution.

Let δt be the duration of the pulse obtained after time reversal (i.e., the correlation time of the transmitted signal) and ΔT the typical duration of the transmitted intensity $|h(t)|^2$ (within the diffusion approximation, ΔT grows proportionally to L^2). We have $\Delta T \propto 1/\delta\omega$ and $\Delta\omega \propto 1/\delta t$, so the number N_T of ''information grains'' grows with L and may be expressed in the time or in the frequency domain as

$$N_T = \Delta T/\delta t = \Delta\omega/\delta\omega \propto L^2. \quad (30)$$

E. Ergodicity and long-range correlation

By how much is it possible to enlarge N_T? Is it possible to obtain an arbitrarily low background level? To that end, we have to increase N_T as much as possible by enlarging the sample thickness L. But then we have to tackle the problem of ergodicity: the amount of information available from one realization of disorder is not infinite.

If the sample thickness L is increased, then the ''time of flight'' distribution spreads over a longer duration since $\Delta T \propto L^2$, and the spectral correlation length $\delta\omega$ decreases. As long as the bandwidth $\Delta\omega$ remains constant, then the number of information grains increases too. But we have seen that when the sample thickness becomes too large, temporal sidelobes appear in the time-reversed signals (i.e., the correlation time δt of the scattered signals increases), which implies that the frequency bandwidth $\Delta\omega$ decreases. Hence the number of information grains must reach a limit. Physically speaking, what happens is that as the sample thickness increases, there

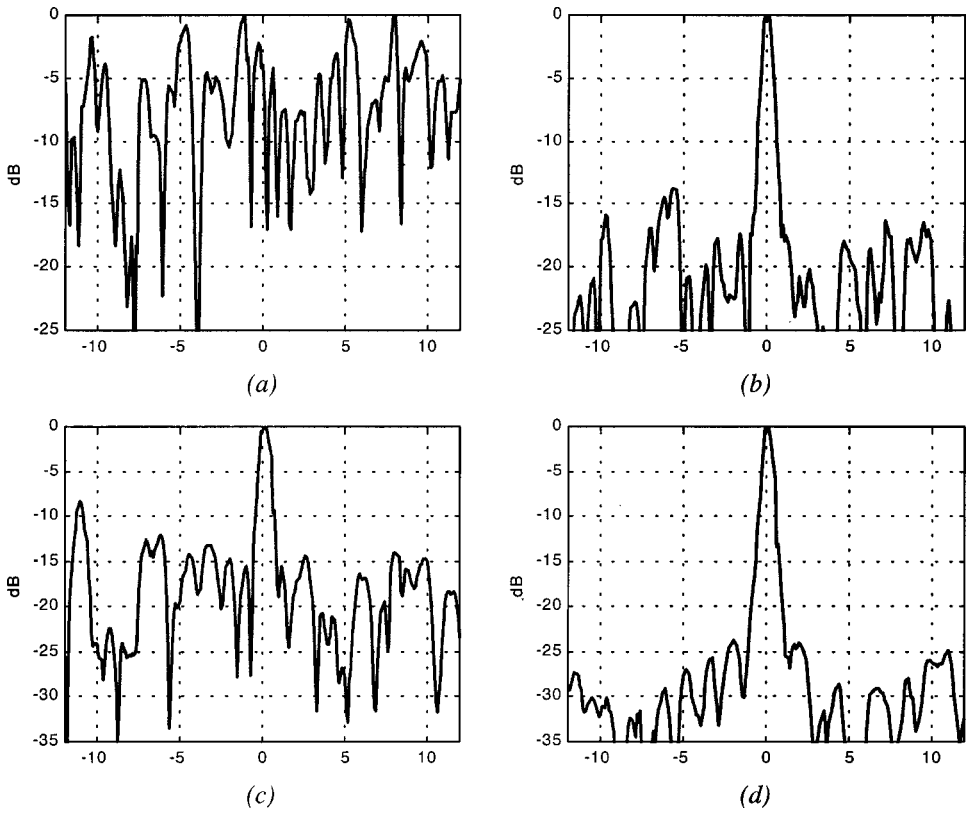

FIG. 10. Directivity patterns through $L=40$ mm (abscissa: distance from the source in mm). (a) Phase conjugation, one element, (b) Time reversal, one element, (c) phase conjugation 128-element array, and (d) time-reversal 128-element array.

are more and more possible scattering paths going from the source to the receiver, but these paths tend to be more and more intricate and in the long run, they all are somewhat correlated.

Yet there is another way to lower the fluctuations of the directivity pattern: it consists of using a whole set of receivers (an array) instead of performing the time-reversal operation on a single element. For simplicity, imagine that the source is at some point P_1; the time-reversal operation is performed on two elements R_1 and R_2, and the time-reversed wave is sensed at a point P_2, off the source by a few wavelengths. Both R_1 and R_2 contribute to a focusing peak at the source. The key issue for the background level of the directivity pattern is to know whether their contribution outside the source adds constructively or destructively. This amounts to evaluate the correlation between $H(R_1 \rightarrow P_1)H^*(R_1 \rightarrow P_2)$ and $H(R_2 \rightarrow P_1)H^*(R_2 \rightarrow P_2)$. If the scattered field has a finite coherence length δx, and the array elements R_1 and R_2 are apart by a distance larger than δx, then the fields are decorrelated. This time, the number of relevant ''information grains'' is the ratio of the array aperture ΔX to the coherence length δx of the scattered field. As before in the case of time correlations, it can also be expressed in the dual k space:

$$N_s = \Delta X / \delta x = \Delta k / \delta k, \tag{31}$$

N_S, as N_T, can be expected to saturate because of correlated paths.

On the whole, the total number of ''information grains'' is

$$N = N_T \times N_S \tag{32}$$

and the fluctuations of the directivity pattern should decrease by $\sqrt{N}$ when the time-reversal operation is performed on a wide frequency band with a large aperture instead of a single frequency and a single element. Figure 10 shows how the background level of the directivity pattern is lowered when N is enlarged, both frequency- and space-wise.

When we do a phase-conjugation experiment with a single element [Fig. 10(a)], the fluctuations around the source are of the same order than the amplitude at the source, so no focusing is visible. As the number of information grains is increased (either by enlarging the bandwidth or the number of array elements) the focusing gets better (Fig. 10). When 128 transducers are used instead of one, the background level is decreased by 15 dB (5.6 on a linear scale), and it is decreased by another 15 dB when using the full bandwidth ($\sim$2–4.5 MHz) instead of a single frequency. This means that $N_T \cong N_S \cong 5.6^2 = 30$, hence the total number of information grains is $N \sim 900$.

Since there are 128 subwavelength elements on the array, we could have expected a number of ''spatial information grains'' larger than 30. Figure 11 displays the background level [according to the definition of the directivity pattern specified by Eq. (12)] versus the number of adjacent elements performing the time reversal. Initially, the background level decreases as the inverse square root of the number of transducers, as expected if the scattered field had a finite correlation length δx; then it seems to saturate around -28 dB. Particularly, enlarging the aperture from 64 to 128 transducers brings no significant improvement, as if all the necessary information was contained on the 64 central transducers. As a whole, when the aperture is increased from 1 to 128

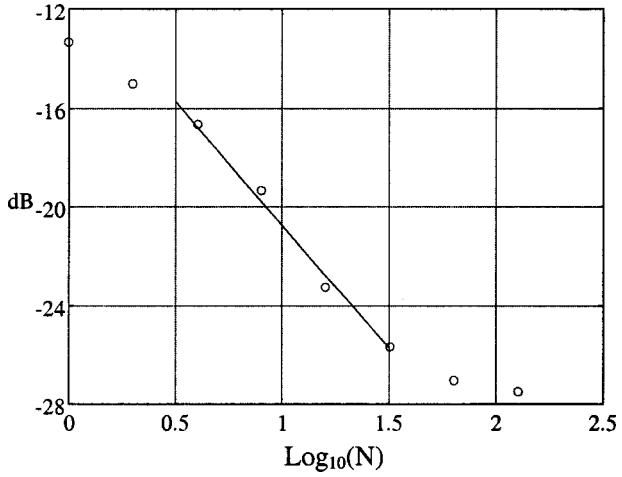

FIG. 11. ($L=40$ mm) Background level of the directivity pattern (in dB) versus the number N of transducers. In the central part of the plot (linear fit), as N is multiplied by 10 the background decreases by 10 dB, as expected from the $\sqrt{N}$ dependency. But for values of N larger than 64 elements, the curve seems to saturate around -28 dB.

transducers, the background level is lowered by roughly 15 dB (5.6 on a linear scale), which confirms the previous estimation $N_S \sim 5.6^2 \sim 30$.

The obvious redundancy of information on the array and the finite number of independent information at a given frequency evokes the question of long-range correlation that has been pointed out in other fields of wave physics. In every multiple scattering problem, in addition to the mean free paths and the diffusion constant, there is another fundamental parameter: the Thouless number, also known as the dimensionless conductance g. In a disordered mesoscopic sample (e.g., a disordered metal for electron propagation, or a waveguide with random scatterers for optical waves) the dimensionless conductance is

$$g = \sum_{a,b} T_{ab}, \tag{33}$$

where T_{ab} denotes the intensity transmission coefficient through the sample from a propagating wave-guide mode (or ''channel'') a to another mode b. In quantum physics as well as in optics, these ''channels'' can be thought of as the various quantized directions along which a wave packet goes in or out of the sample.

In our case, g can be roughly estimated by the number of incoming ''channels'' multiplied by the conductance of a given channel:

$$g \approx \frac{W l^*}{\lambda L}, \tag{34}$$

where W is the width of the incoming beam and λ its wavelength, l^*/L being as usual the average ratio of intensity transmitted through the sample.

Interestingly, this quantity can be related to the performance of a time-reversal device in a multiple scattering environment. Indeed the Thouless factor g can also be interpreted as the number of independent parameters which are needed to represent a monochromatic wave in a random medium [4]. Therefore measuring the maximum number of ''spatial information grains'' N_S via a time-reversal experiment is a way to estimate g. From the results above, we conclude that $g = N_S \sim 30$ for $L = 40$ mm. This value is in agreement with the rough estimate that can be derived from Eq. (34): in a typical experiment for $L = 40$ mm we have $W \sim 100$ mm, $\lambda \sim 0.5$ mm, and $l^* = 4.8$ mm, which yields $g \sim 24$. This confirms that we are far from the ''mobility edge,'' i.e., the threshold of strong localization, which is believed to occur when g is close to 1.

The value of g determines the number of uncorrelated information that is available in the scattered field. Numerous authors [1–4,15,16,28,29] have pointed out the existence of long-range correlation in optics, when the order of scattering involved becomes very large. They have shown that the intensity–intensity correlation function can be written as a sum of three terms: a short-range [such as C_{12} in Eq. (21)], a long-range, and an infinite range term, with relative ratios, 1, $1/g$, and $1/g^2$. The constant $1/g$ gives an indication of the importance of these long-range correlations. $1/g$ is also shown to be the probability for two paths to intersect within the sample.

These theoretical analysis are consistent with what we observed experimentally. When we do a time-reversal experiment, the signal obtained at the source can be considered as an estimate of the field–field correlation function in time, and the directivity pattern around the source can be considered as an estimate of the field–field correlation function in space. If all correlations, in time and in space, had a finite length (δt in time, δx in space) then by enlarging the array aperture or the sample thickness, the number N of independent information would increase indefinitely, and as result the time-reversed field would statistically converge to a finite pulse with duration δt and spatial extension δx, with an ever reduced variance. But by enlarging the sample thickness, the complexity of the scattering paths gives rise to long range correlation, which, even though their level is only $1/g$, drastically limit the effective number of independent information. The performance of time-reversal focusing is therefore limited by the existence of long-range correlations, measured by the universal parameter g.

Long-range correlation is an important issue *per se* in all kinds of wave scattering, whether quantum or classical. From a more down-to-earth point of view (what should an experimentalist do to obtain the best focusing with a given bandwidth and a given transducer array?) beyond a certain limit (which seems to be 5–10 times the transport mean free path in our case), increasing the sample size does more harm than good in terms of time-reversal focusing.

F. Dynamic time reversal

So far we have shown how the quality of focusing was affected by the frequency bandwidth or the aperture of the time-reversal mirror when all the information that was collected on the array was sent back. But a time-reversal device

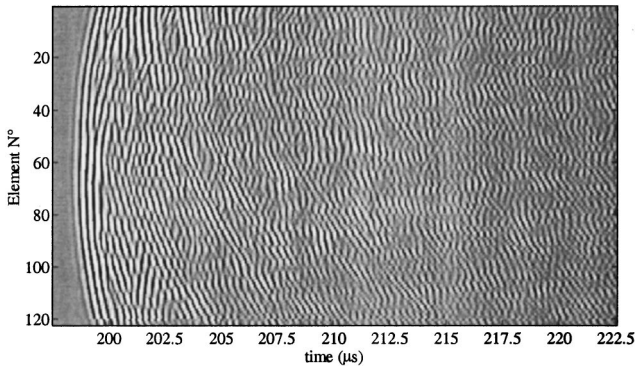

FIG. 12. *B*-scan of the 128 signals received on the array through a multiple scattering sample ($L=15$ mm). The ballistic front is clearly visible for this thickness.

can do more than that: we can easily select a short time window among the scattered signals, and only reverse and send back this portion of the signals. This process is termed ''dynamic time reversal,'' and we will show that the position of the time window has a dramatic impact on the quality of focusing.

We have argued that the spatial resolution of a time-reversal device essentially depends on the correlation length of the scattered wave field: the shorter the coherence length, the finer the resolution. This can be illustrated by dynamic time reversal through a sample of width $L=15$ mm. The scattered signals received on the array are represented in Fig. 12. In a relatively thin sample (here, $L\sim 3l^*$) such as this one, the so-called ''ballistic front'' is clearly visible. Therefore, at early times, the signals received on various elements of the array are strongly correlated. After the ballistic front has arrived, the array continues receiving signals corresponding to scattered waves. Late arrivals correspond to longer scattering paths and a higher order of scattering.

Figure 13 shows the directivity patterns that were obtained with a 64-element aperture by time reversing either the early arrivals or later arrivals. We selected two 2-μs time

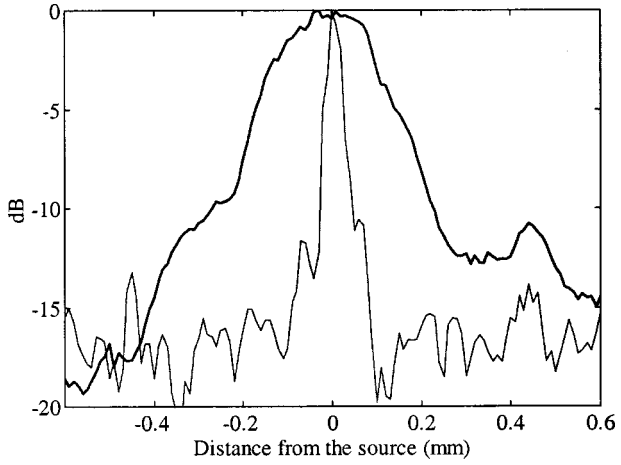

FIG. 13. Directivity patterns obtained after time reversing a 2-μs time window at early times (ballistic front) or at later times (multiple scattering contribution). The spatial resolution is 3.6 mm at early times, 0.5 mm at later times.

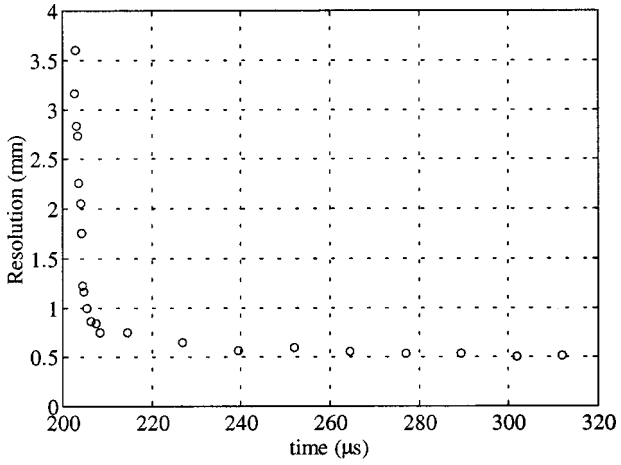

FIG. 14. Spatial resolution versus the beginning time of the time-reversal window, for 2-μs time windows through $L=15$ mm.

windows: the first one including the ballistic front and the second one beginning 100 μs later, i.e., containing purely multiple scattering contributions. The -6 dB resolutions we obtained are 3.6 mm for early arrivals and only 0.5 mm for late arrivals (it should be noted that the average wavelength is 0.47 mm). It appears that at early times, as in a homogeneous medium, the resolution of the system is limited by the aperture of the array. Whereas at later times, multiple scattering dominates, and the resolution is essentially limited by the coherence length of the scattered field.

The evolution of the spatial resolution versus the beginning of the time-reversal window is plotted in Fig. 14. Right after the ballistic front, the resolution diminishes quite sharply down to $\sim$0.5 mm, which seems to be the smallest value that can be attained given the average wavelength (0.45 mm) and the size of our elements (0.39 mm).

Interestingly, the improvement in resolution is not instantaneous: it takes roughly 10 μs to reach the plateau. We think that this transition time is linked to the presence of the resonant ''tail'' in the coherent part of the transmitted wave that lasts longer than the ballistic pulse as was shown in the previous article. The finest resolution can only be obtained when the ''incoherent'' regime is really attained, i.e., when the coherent part $\langle h(t)\rangle$ of the scattered wave is dominated by the ''incoherent'' contribution $n(t)$.

IV. CONCLUSION

The results presented in this article show the following points.

(1) Even in the presence of high-order multiple scattering, a finite-size time-reversal mirror manages to focus a pulse back to the source with a spatial resolution that beats by far the diffraction limit and is only limited by the spatial correlation of the scattered field.

(2) Successful time-reversal focusing on a single element is possible, whereas phase conjugation on a single element completely fails. The efficiency of broadband time reversal compared to monochromatic phase conjugation lies in the number N_T of ''information grains'' in the frequency bandwidth.

(3) When time reversal is performed with an array, the quality of focusing (background level) is enhanced proportionally to $\sqrt{N_S}$, where N_S is the number of ''spatial information grains'' on the array aperture.

(4) As the sample thickness becomes very large compared to the transport mean free path, correlations between the scattering paths result in a saturation of both N_S and N_T: persistent secondary sidelobes in the temporal wave form appear, and increasing the array aperture does no longer enhance the quality of focusing. The maximum value of N_S is the number of independent parameters which are needed to represent a monochromatic wave in a random medium, i.e., the Thouless number g.

(5) Despite long-range correlation, the total number of ''information grains'' through a slab with thickness $L \sim 8l^*$ is found to be $N_T \times N_S \sim 900$, which is enough to ensure that one realization of disorder suffices to get a robust estimation of the time and space correlation functions from a single realization of disorder. In that sense, time reversal is a ''self-averaging'' process.

(6) If one wants to exploit time reversal in a multiple scattering environment in order to have the best resolution possible then one should choose L/l^* large enough to kill the coherent wave, but small enough to avoid long-range correlation. In our case, a satisfying compromise seems to be $L \sim 5l^*$.

(7) On the contrary, if time reversal is employed as a tool to study long-range correlation, it might be interesting to rearrange the rods in such a way that g is decreased, and brought closer to 1. From the previous analysis, the quality of time-reversal focusing would be degraded, until the moment (mobility edge) where the results will be as bad as phase conjugation, which means there would be only one ''information grain.'' This remains an experimental challenge.

[1] P. Sheng, *Introduction to Wave Scattering, Localization and Mesoscopic Phenomena* (Academic, New York, 1995).

[2] A. Lagendijk and B. A. Van Tiggelen, Phys. Rep. **270**, 143 (1996).

[3] M. C. W. van Rossum and T. M. Nieuwenhuizen, Rev. Mod. Phys. **71**, 313 (1999).

[4] A. Z. Genack, in *Scattering and Localization of Waves in Random Media*, edited by P. Sheng (World Scientific, Singapore, 1990), pp 207–311.

[5] P. A. Lee and T. V. Ramakrishnan, Rev. Mod. Phys. **57**, 287 (1985).

[6] L. Margerin, M. Campillo, and B. van Tiggelen, Geophys. J. Int. **134**, 596 (1998).

[7] A. Tourin, M. Fink, and A. Derode, Waves Random Media **10**, R31 (2000).

[8] D. E. Khmelnitskii, Physica B **126**, 235 (1984).

[9] Y. Kuga and A. Ishimaru, J. Opt. Soc. Am. A **1**, 831 (1984).

[10] M. P van Albada and A. Lagendijk, Phys. Rev. Lett. **55**, 2692 (1985).

[11] E. Wolf and G. Maret, Phys. Rev. Lett. **55**, 2696 (1985).

[12] E. Akkermans, P. E. Wolf, R. Maynard, and G. Maret, J. Phys. **49**, 77 (1988).

[13] A. Tourin, A. Derode, P. Roux, B. A. Van Tiggelen, and M. Fink, Phys. Rev. Lett. **79**, 3637 (1997).

[14] T. Niederdränk *et al.*, Phys. Rev. Lett. **70**, 3884 (1993).

[15] F. Scheffold, W. Härtl, G. Maret, and E. Matijevic, Phys. Rev. B **56**, 10942 (1997).

[16] D. S. Wiersma, P. Bartolini, A. Lagendijk, and R. Righini, Nature (London) **390**, 671 (1997).

[17] J. de Rosny, A. Tourin, and M. Fink, Phys. Rev. Lett. **84**, 1693 (2000).

[18] M. Fink *et al.*, Rep. Prog. Phys. **63**, 1933 (2000).

[19] M. Tanter, J.-L. Thomas, and M. Fink, J. Acoust. Soc. Am. **103**, 2403 (1998).

[20] W. A. Kuperman *et al.*, J. Acoust. Soc. Am. **103**, 25 (1998).

[21] V. Miette *et al.*, *Proceedings of the IEEE Ultrasonic Symposium, San Antonio, TX, 1996* (IEEE, New York, 1996).

[22] C. Draeger and M. Fink, J. Acoust. Soc. Am. **105**, 611 (1999).

[23] C. Draeger, J.-C. Aime, and M. Fink, J. Acoust. Soc. Am. **105**, 618 (1999).

[24] A. Derode, A. Tourin, and M. Fink, J. Appl. Phys. **85**, 6343 (1999).

[25] P. Blomgren, G. Papanicolaou, and H. Zhao, J. Acoust. Soc. Am. (to be published).

[26] A. Derode, P. Roux, and M. Fink, Phys. Rev. Lett. **75**, 4206 (1995).

[27] A. Tourin, A. Derode, A. Peyre, and M. Fink, J. Acoust. Soc. Am. **108**, 503 (2000).

[28] B. Shapiro, Phys. Rev. Lett. **57**, 2168 (1986).

[29] R. Berkovits and S. Feng, Phys. Rep. **238**, 135 (1994).